



Cite this: *Inorg. Chem. Front.*, 2024, **11**, 3119

# Surface functionalization of metal–organic framework nanoparticle for overcoming biological barrier in cancer therapy

Jun Yong Oh,<sup>†a</sup> Youjung Sim,<sup>†a</sup> Gyeongseok Yang,<sup>†a</sup> Myoung-Hwan Park,<sup>id</sup>\*<sup>b</sup> Kibeom Kim\*<sup>b</sup> and Ja-Hyoung Ryu<sup>id</sup>\*<sup>a</sup>

Nanomedicine, which merges the realms of nanotechnology and medicine, presents transformative strategies for advancing healthcare through nanoscale manipulation of materials. Among these, metal–organic frameworks (MOFs), with a unique hybrid structure of metal ions interconnected by organic ligands, have emerged as a novel class of inorganic nanoparticles with significant potential in drug delivery systems (DDS). This review explores the innovative applications of MOFs in DDS, emphasizing their distinctive porous architectures that facilitate the adsorption and controlled release of therapeutic agents. The versatility of MOFs is further enhanced by surface functionalization, which not only augments their dispersibility and targeting efficiency but also addresses the biological barriers that traditionally impede nanoparticle-based drug delivery. These barriers include the adsorption of bioproteins, which can mask the nanoparticles and prompt immune recognition, and the complex interplay within the tumor microenvironment (TME), which affects nanoparticle penetration and efficacy. Additionally, the cell membrane prevents nanoparticles from being internalized into the cell, and drugs released within the cell are removed by efflux pumps, impeding their therapeutic effect. Through a comprehensive analysis, we highlighted the strategies employed to overcome these obstacles, leveraging the multifunctional capabilities of MOFs to enhance their therapeutic payload delivery and targeting precision.

Received 27th February 2024,  
Accepted 20th April 2024

DOI: 10.1039/d4qi00523f

rsc.li/frontiers-inorganic

## Introduction

Nanomedicine, a ground-breaking field at the crossroads of nanotechnology and medicine, has ushered in a new era of possibilities for diagnosing, treating, and understanding diseases at the nanoscale.<sup>1</sup> Inorganic nanoparticles are a key to the progress of nanomedicine. They exhibit unique properties and versatile functionalities that hold immense promise in various scientific and technological domains, offering unique properties and capabilities that hold immense potential for revolutionizing healthcare.<sup>2–5</sup> In this context, a prominent class of inorganic nanoparticles has garnered significant attention as a framework for drug delivery systems (DDS), such as metal–organic frameworks (MOFs).

MOFs represent a captivating class of crystalline materials composed of metal ions or clusters linked by organic ligands.<sup>6–9</sup> This unique hybrid composition led to the formation of porous structures with remarkable tunability in

terms of pore size, geometry, and chemical functionality.<sup>10–14</sup> The unprecedented diversity in MOF design and synthesis has opened up avenues for applications spanning gas storage and separation, catalysis, drug delivery, and even electronic devices.<sup>15–17</sup> The large internal surface area of MOFs provides ample space for guest molecules to adsorb, making them ideal for gas storage and cargo loading.<sup>18,19</sup>

The promising possibilities of MOF particles are maximized through surface functionalization.<sup>20–22</sup> Surface chemistry delves into the interactions between molecules to create larger organized structures held together by various conjugation pathways. This dynamic approach exploits the reversible and highly specific nature of these interactions, allowing the design of complex architectures and functional systems. This process involves the controlled assembly of nanoparticles with complementary molecules (targeted ligands)<sup>18,19</sup> or macromolecules (proteins and polymers)<sup>23,24</sup> through various interactions.<sup>25–29</sup> Nanoparticles with improved dispersibility and targeting capabilities can be engineered by selecting appropriate functional materials.

Nonetheless, the incorporation of MOF-based drug delivery systems within biological environment necessitates a comprehensive comprehension, as delineated in the review by Wang *et al.*<sup>30</sup> Upon introduction into the environment, nanoparticles

<sup>a</sup>Department of Chemistry, Ulsan National Institute of Science and Technology, Ulsan 44919, Republic of Korea. E-mail: jhryu@unist.ac.kr

<sup>b</sup>Department of Chemistry and Life Science, Sahmyook University, Seoul, 01795, Republic of Korea. E-mail: mpark@syu.ac.kr, kibumsy@syu.ac.kr

<sup>†</sup>These authors contributed equally to this work.



undergo systemic circulation within the bloodstream, interacting with a myriad of bioproteins. The adherence of these bioproteins to the nanoparticle surface can compromise their diverse functionalities.<sup>31</sup> Specifically, if attachment occurs with immune-related proteins, the nanoparticles become susceptible to immunological recognition, leading to their subsequent elimination or filtration by specific organs.<sup>32</sup> Consequently, it is imperative to develop methodologies aimed at minimizing the adsorption of bioproteins onto nanoparticle surfaces to facilitate prolonged circulation within the biological milieu. Next, the tumor microenvironment (TME) plays a pivotal role, orchestrating a dynamic interplay of cellular, molecular, and structural components that collectively influence the fate and behavior of tumors.<sup>33</sup> This complex ecosystem extends beyond cancer cells, encompassing stromal cells, immune cells, blood vessels, and extracellular matrix components, and decisively regulates key aspects of tumorigenesis, progression, and response to therapy.<sup>34</sup> The understanding of intricate crosstalk within the TME has paved the way for targeted therapeutic interventions. The dynamic nature of TME components, including a low pH, high GSH level, and hypoxia, offers a rich landscape for potential therapeutic strategies, ranging from immunomodulation to targeting angiogenesis and disrupting stromal interactions.<sup>35</sup> In addition, for nanoparticles to ingress into cellular interiors, they must traverse the cell membrane, wherein the physicochemical attributes of the cell membrane dictate the permeability of said nanoparticles.<sup>36</sup> Specifically, the internal transport of nanoparticles can be facilitated through interaction with specific receptors situated on the cell membrane.<sup>37</sup> However, incongruities in size, shape, charge, and polarity, as well as the exocytosis and push-back mechanisms inherent to the cell membrane, pose

impediments that may hinder particle delivery.<sup>38,39</sup> Consequently, the reciprocal interplay between the characteristics of nanoparticles and properties of the cell membrane intricately governs the efficiency of nanoparticle delivery and exerts influence over specific biological responses. This comprehensive understanding will contribute to the optimization of nanoparticle technology utilization across diverse applications, notably within the realms of medicine and drug delivery. In this review, we explore drug delivery systems based on MOF nanoparticles *via* various surface functionalization methods to overcome these biological barriers (Scheme 1). Their tailored properties and multifunctional capabilities offer unprecedented opportunities for enhancing diagnostics, drug delivery, and therapy. Specifically, the diverse configurations of MOF nanoparticles offer a spectrum of potentialities, enhancing the versatility of platforms to encompass not only two-dimensional but also three-dimensional therapeutic modalities.<sup>40</sup> This investigation aimed to recognize the bioenvironmental challenges encountered in drug delivery systems incorporating MOF nanoparticles to provide insights into efficacious strategies for mitigating these challenges. Such endeavors serve as pivotal indicators in shaping the trajectory of the prospective development of drug delivery systems that leverage MOF nanoparticles.

## Clearance and biodistribution

When MOF nanoparticles are injected intravenously into the body for cancer therapy, the body clearance system is the first biological barrier encountered. Body clearance occurs through phagocytosis based on the immune system as well as filtration



**Scheme 1** Surface functionalization of MOF nanoparticle for overcoming biological environment, tumor microenvironment, and cellular internalization.



at certain organs while circulating in the bloodstream.<sup>41</sup> This leads to the elimination of external substances such as MOF nanoparticles by the reticuloendothelial (RES) system.<sup>42</sup> Therefore, one of the objectives of achieving adequate cancer therapeutic effects is maintaining appropriate biodistribution to reach the target cancer without being detected by the clearance system (Fig. 1A).

The RES system operates in filtration and immune organs such as the liver and lymph nodes. The mononuclear phagocytic system (MPS) induces clearance by certain immune cells such as monocytes and macrophages in these organs.<sup>43</sup> One way of avoiding biological conditions is to “camouflage”. A cell membrane coating was adopted for the surface modification of the MOF nanoparticles to enhance blood circulation in the *in vivo* phase.

First, Cheng *et al.* reported a system that could evade the immune system using zeolitic imidazolate framework (ZIF-8) MOF nanoparticles decorated with an extracellular vesicle (EV) membrane (Fig. 1B).<sup>44</sup> The extracellular vesicle could involve integrin-associated transmembrane protein CD 47, which shows “do not eat me” signals to evade phagocytosis.<sup>45</sup> EVs were collected with ultracentrifugation, only the extracellular

vesicle membrane (EVM) was extracted by hypotonic treatment, and over 97% of the MOF nanoparticles were decorated. The reduced opsonization and phagocytosis-based clearance were confirmed by incubation with fluorescent immunoglobulin G, achieving reduced fluorescent 6-fold for the bare MOF and 4-fold for the liposome-enveloped MOF. In addition, after encapsulation with fluorescent proteins, the EVM-coated MOF showed a significant decrease in the fluorescence of RAW264.7 macrophage cell internalization, as confirmed by confocal laser scanning microscopy (CLSM), flow cytometry, and quantification of mean fluorescence intensity. Hence, the results demonstrate EVM with the functions of biomimetic camouflage, phagocytosis evasion, and prolonged circulation of MOF nanoparticles.

In a different study, Zhang *et al.* reported biomimetic and glucose oxidase-loaded MOF systems that can enhance clearance stability and circulation, using ZIF-8 MOF nanoparticles and modification with erythrocyte membrane (eM) (Fig. 1C).<sup>46</sup> The authors intended to use nature's erythrocyte membrane for camouflage of the MOF nanoparticles, using characteristics of RBC, which can be survived approximately 115 days under blood circulation.<sup>47</sup> The eM-coated MOF nanoparticle loading



**Fig. 1** (A) Schematic of MOF NPs overcoming biological environment. (B) Schematic of EMF (Extracellular vesicle-MOF-protein) nanoparticles preparation. 1: MOF-protein (MP) nanoparticle preparation by self-assembly of organic ligand, metal ions, and caging protein cargo. 2: Extraction of extracellular vesicle membrane (EVM). 3: EMF nanoparticle EVM modification on the MP nanoparticle surface. Reproduced with permission.<sup>44</sup> Copyright (2018): American Chemical Society. (C) Schematic of TGZ@eM nanoreactor preparation; TGZ@eM is an erythrocyte membrane cloaked MOF-based biomimetic nanoreactor. For the synthesis of the MOF,  $Zn^{2+}$  and 2-methylimidazole were chosen as the metal ion and organic ligand, respectively. Reproduced with permission.<sup>46</sup> Copyright (2018): American Chemical Society.



with rhodamine B was observed with only dim red fluorescence treated to RAW 264.7 cell; however, eM uncoated MOF was detected under bright red fluorescence. Moreover, *in vivo* pharmacokinetic curves confirmed the enhanced blood circulation half-life of the eM-MOF, which was two times longer than that of the bare MOF. Hence, the results also demonstrated that erythrocytes function as a biomimetic camouflage and enhance blood circulation to MOF nanoparticles.

In nanomedicine, the protein corona phenomenon is the formation of a layer onto the surface of nanomedicine when injected into the biological system, which has abundant protein types.<sup>48</sup> This phenomenon changes the characteristics of nanomedicine, such as size and charge, leading to a decrease in blood circulation time and opsonization to be cleared.<sup>49</sup> Attempts to modify nanomedicine interfaces have been made to enhance stability against protein adsorption and increase efficiency as a drug delivery system.

First, Zhang *et al.* reported a system that presents highly stable and long-circulating *in vivo* properties, using a UiO-66 MOF that is surface-functionalized with a 1,2-dioleoyl-*sn*-glycero-3-phosphate (DOPA) lipid bilayer (LB).<sup>50</sup> Facile one-step sonication induces covalent linkage between the terminal of DOPA and the UiO-66 surface, forming a Zr–O–P coordination bond between the metal and phosphate. In addition to the use of conventional polyethylene glycol (PEG) on MOF nanoparticles, the stealth effect of evading mononuclear phagocytic clearance can be achieved by introducing LBs. Regarding the long-circulation property, the half-life was observed to be 4 h for UiO-66@DOPA-LB, whereas it was 0.5 h for UiO-66-PEG.

Hence, the results demonstrated an enhanced biodistribution property, achieving facile functionalization of the MOF nanoparticle system by the DOPA lipid bilayer.

Zimpel *et al.* investigated the behavior of zirconium–fumarate (Zr-fum) MOF nanoparticles while controlling the coordinative binding between the polymer and MOF interfaces.<sup>29</sup> The different types of polymers confirmed their capacity for protein binding and cellular association under biological conditions. The cellular association and uptake profile were observed by CLSM and flow cytometry. Zr-fum@PGLu-PSar (zirconium-fumarate@polyglutamate-*b*-polysarcosine) was selected to demonstrate the serum stability for cellular association. The polysarcosine (PSar) copolymer with PGLu could achieve a shielding effect and colloidal stabilization properties similar to those of PEG by multiple hydrogen bonding. PSar is considered to be a less immunogenic alternative and a shielding agent that enhances circulation lifetimes. In addition, the fluorescence intensity was observed as a biodistribution in the liver after 24 h in mice injected with Zr-fum@Cy5.5-PGLu-PSar. This result demonstrates that polymer functionalization differs between the MOF interfaces and their biological fates.

Tian *et al.* reported a system that achieves extended blood circulation time by inhibiting the accelerated blood clearance (ABC) phenomenon. They used ZIF-8 MOF-based nanoparticles, which are crosslinked by 8-arm-PEG-TNB (8-arm-PEG-2-nitro-5-thiobenzoate) and further modified with hyaluronic acid (Fig. 2A).<sup>51</sup> The PEG NPs were synthesized by combining zinc nitrate solution, 2-methylimidazole (2-MIM) as an organic linker, sequential disulfide crosslinking with 8-arm-PEG-TNB, 8-arm-PEG-SH *via* thiol-disulfide exchange, and

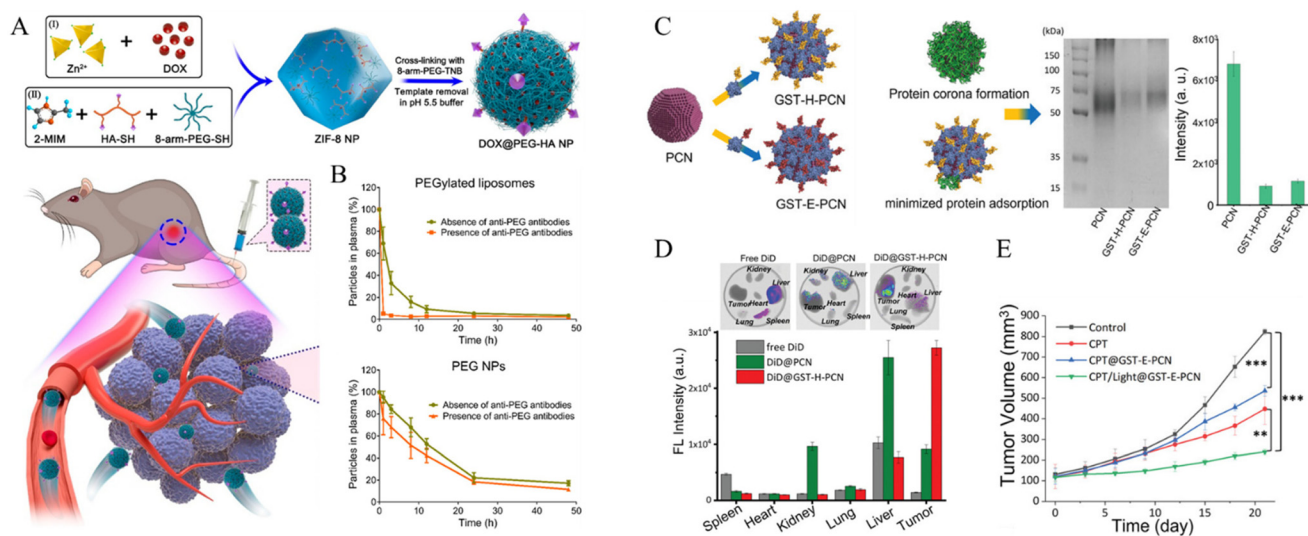


**Fig. 2** (A) Schematic of PEG NPs based on ZIF-8 NPs, mixing zinc nitrate, 2-methylimidazole, 8-arm-PEG-SH, thiolated HA, and crosslinking with 8-arm-PEG-2-nitro-5-thiobenzoate and template removal. (B) Schematic pharmacokinetics examination of PEGylated liposomes and PEG. Circulation times from PEGylated liposomes and PEG in the absence and presence of anti-PEG antibodies. Reproduced with permission.<sup>51</sup> Copyright (2022): American Chemical Society. (C) Gel electrophoresis for evaluation of protein corona inhibition property of bare PCN-224, GST-Afb precoated PCN-224. Resulting intensities of protein band quantification decreased 7.5-fold for GST-H-PCN and 6.7-fold for GST-E-PCN compared with PCN. (D) Fluorescence imaging of tumor and organs for intravenously injected dye-related materials. (E) Tumor volume change and weight measurement for inhibition experiment by drug-loaded nanoparticle with therapeutic application. Reproduced with permission.<sup>52</sup> Copyright (2023): John Wiley and Sons.



finally, template removal under acidic condition to construct stealth nanoparticles for enhanced biodistribution. In this study, rapid clearance *via* the ABC phenomenon was prevented by decreasing protein adsorption and immune cell interactions. The 8-arm-PEG could achieve low protein adsorption owing to its highly hydrated properties under serum protein conditions. Immunogenicity due to the secretion of anti-PEG antibodies is one of the main factors in ABC. The authors observed that anti-PEG antibodies were not produced in the nanoparticle, whereas other PEGylated groups were detected. Considering these results, a pharmacokinetic study for biodistribution evaluated the effect of immunogenic antibodies on circulation time. The PEGylated liposomes significantly cleared in the presence of anti-PEG antibodies. In contrast, the synthesized nanoparticles demonstrated minimal clearance and achieved a prolonged circulation half-life of 12 h (Fig. 2B).

Oh *et al.* developed a system that could inhibit the protein corona phenomenon using a pre-coating of glutathione *S*-transferase-fused targetable affibody (GST-Afb) onto a Zr6-based MOF (PCN-224).<sup>52</sup> Protein corona inhibition was confirmed by gel electrophoresis, exhibiting a minimized serum protein signal approximately 7-fold lower than that of the bare MOF (Fig. 2C). Moreover, the composition of serum proteins adsorbed onto GST-Afb-PCNs was quantified by liquid chromatography-tandem mass spectrometry (LC-MS/MS). Immune response-related proteins, such as complement proteins, were detected at significantly lower levels, demonstrating that GST-Afb enables MPS evasion against the immune system and longer biodistribution of MOF nanoparticles. GST-Afb proteins were stably functionalized onto the surface of the MOF, as confirmed by molecular dynamics simulations between GST-Afb and the MOF surface, maintaining a certain orientation for cell-targeting Afb to be exposed outward. Moreover, a targeting effect was observed in both *in vitro* and *in vivo* systems. The GST-Afb MOF loaded with a fluorescent dye selectively targeted tumor accumulation in xenografted tumors by *in vivo* imaging. Moreover, the tumor inhibition experiment confirmed 71% tumor suppression by the photodynamic therapy-associated GST-Afb MOF system (Fig. 2D and E). These results demonstrate that the system can simultaneously target cells and prevent protein corona formation.

## Tumor microenvironment

As previously delineated, comprehension of the TME is imperative for the efficacious delivery of therapeutic agents. In this section, we elucidate the intricacies of the TME concerning platforms designed to either respond to or surmount its challenges. Furthermore, we explore pertinent research endeavors aimed at exploiting and overcoming these challenges. This complex ecosystem extends beyond cancer cells, encompassing stromal cells, immune cells, blood vessels, and extracellular matrix components, and decisively regulates key aspects of tumorigenesis, progression, and response to therapy.<sup>53</sup> The understanding of intricate crosstalk within the

TME has paved the way for targeted therapeutic interventions. The dynamic nature of the TME components, such as low pH, high glutathione (GSH) levels, hypoxic conditions, and dense extracellular matrix (ECM), offers a rich landscape for potential therapeutic strategies, ranging from immunomodulation to targeting angiogenesis and disrupting stromal interactions.<sup>54</sup>

An increasingly recognized factor within this multifaceted milieu is the pH of the TME. Marked by its acidic nature, characterized by a lower extracellular pH compared to the surrounding normal tissues, it stands out as a distinctive feature with profound implications for tumorigenesis, metastasis, and treatment outcomes.<sup>55</sup> This acidity results from altered metabolic processes in cancer cells, leading to the accumulation of acidic byproducts, such as lactate and protons. Beyond reflecting the metabolic adaptations of cancer cells, this acidic microenvironment plays a pivotal role in shaping the behavior of both malignant and stromal cells within the TME.<sup>56</sup>

GSH has emerged as a key contributor influencing redox balance, cellular signaling, and therapeutic responses within the TME. GSH, a tripeptide composed of glutamate, cysteine, and glycine, is the principal antioxidant that maintains cellular redox homeostasis. In the TME, alterations in GSH levels and redox status shape the fate of cancer cells, regulate intracellular signaling pathways, and modulate responses to oxidative stress, DNA damage, and apoptotic signals.<sup>57</sup>

The ECM plays a critical role in providing structural and biochemical support to the cellular components. Understanding and surmounting the challenges posed by the ECM in the TME are paramount for advancing cancer research and therapeutic strategies.<sup>58</sup> The ECM in the TME is characterized by alterations in composition, organization, and mechanical properties, creating a unique niche that influences cellular behavior, angiogenesis, and immune responses. These modifications not only contribute to tumor growth and invasion but also affect the efficacy of anticancer treatments. Conventional therapies often encounter limitations in penetrating dense and heterogeneous ECM, diminishing their effectiveness and fostering treatment resistance.<sup>59</sup>

Finally, the heightened cancer cell proliferation within solid tumors leads to aberrant vascularization, culminating in the development of incomplete neovascular structures in contrast to the well-organized vasculature observed in normal tissues. As the tumor expands, its vascularity increases rapidly, resulting in regions with substantially reduced oxygen levels compared to the adjacent healthy tissues. Oxygen, an indispensable element in dynamic cancer therapies, orchestrates cell death *via* reactive oxygen species and plays a pivotal role in various established cancer treatment modalities. However, these therapeutic interventions experience a discernible decline in hypoxic environments, which imposes significant constraints on their clinical applicability.<sup>60</sup> Consequently, low pH, high GSH concentration, ECM, and hypoxia of the TME have been identified as key modulators of crucial cellular processes, including proliferation, invasion, and immune surveillance (Fig. 3A).

In addition to overcoming the barriers posed by the TME, MOF-based drug delivery systems that use the TME as a trigger



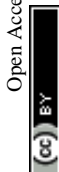


**Fig. 3** (A) Schematic of MOF NPs overcoming tumor microenvironment. (B) Schematic of pH responsive cluster MOF Reproduced with permission.<sup>59</sup> Copyright (2022): John Wiley and Sons. (C) The schematic of construction and the anti-inflammation response of pH responsive MOF nanoparticles. Reproduced with permission.<sup>61</sup> Copyright (2023): Springer Nature.

have been developed. The low pH of the TME can be exploited as a trigger. Considering this, Cheng *et al.* synthesized a pH-responsive linker (L) by covalently modifying oleylamine with 3-(bromomethyl)-4-methyl-2,5-furandione (MMfu) and poly(ethylene glycol) (PEG) (Fig. 3B).<sup>59</sup> Subsequently, the linker (L) was incorporated into a solid lipid nanoshell to encapsulate apilimod (Ap)-loaded ZIF(Ap-ZIF), resulting in the formation of Ap-ZIF@SLN#L. Within the TME, the hydrophilic PEG and MMfu moieties undergo removal, exposing the hydrophobic oleylamine on Ap-ZIF@SLN#L. This modification enhances the uptake of nanoparticles by cancer cells and their subsequent accumulation within the tumors. Ap-ZIF@SLN#L nanoparticles induced the generation of reactive oxygen species (ROS). The Ap released from Ap-ZIF@SLN#L significantly promoted the production of intracellular ROS and lactate dehydrogenase. Overall, this pH-responsive targeting strategy improved nanoparticle accumulation in tumors, leading to enhanced therapeutic effects. In addition, Zhang *et al.* presented a comprehensive investigation involving a pH-responsive MOF, specifically denoted as MIL-101-NH<sub>2</sub> (MIL standing for Material of Institute Lavoisier), designed for the simultaneous co-delivery of the anti-inflammatory agent curcumin (CCM) and small interfering RNA (siRNA) targeted toward hypoxia-

inducible factor-2 alpha (HIF-2α) (Fig. 3C).<sup>61</sup> The loading of both CCM and siRNA onto MIL-101-NH<sub>2</sub> was accomplished through a combination of encapsulation mechanisms and the surface coordination capabilities inherent to MIL-101-NH<sub>2</sub>. These *in vitro* experiments revealed that MIL-101-NH<sub>2</sub> exhibits a pronounced protective effect against siRNA, shielding it from nuclease degradation *via* lysosomal escape. The inherent pH-responsive attributes of MIL-101-NH<sub>2</sub> facilitated a gradual structural collapse within the acidic osteoarthritis microenvironment. This orchestrated collapse leads to the controlled release of CCM payloads, resulting in the downregulation of pro-inflammatory cytokine levels. Simultaneously, MIL-101-NH<sub>2</sub> released siRNA payloads, enabling the cleavage of the target HIF-2α mRNA for gene-silencing therapy. Consequently, the collective therapeutic action of silencing HIF-2α genes was observed, demonstrating a synergistic effect in conjunction with the inhibition of the inflammatory response and mitigation of cartilage degeneration in osteoarthritis.

In addition to the low pH, high GSH levels in the TME can also be used as a trigger. Liu *et al.* developed a core-shell MOF nanoplatform for intelligent GSH imaging and simultaneous GSH reduction, aiming for synergetic photodynamic therapy (PDT) and gene therapy.<sup>56</sup> The nanoplatform, composed of a



porous coordination network (PCN)-typed MOF core and a Cu<sup>II</sup>-centered ZIF-67 (ZIF-67(Cu)) shell, was designed to release cyanine 3 (Cy3)-labeled siRNA upon internalization by cells. The GSH-responsive collapse of the ZIF67(Cu) shell led to intracellular GSH consumption, activating the photosensitized PCN and enabling synergistic therapeutic approaches, including GSH imaging, siRNA-mediated gene therapy, and enhanced PDT with GSH depletion. The abundant generation of ROS further improved gene silencing efficiency by assisting siRNA endosomal escape. This GSH-responsive nanoagent shows promise for maximizing the therapeutic efficacy of PDT with gene therapy, suggesting potential advancements in MOF hybrids for intracellular stimulus-activated theranostics. Du *et al.* synthesized a nanodrug (designated BMS-SNAP-MOF) utilizing a GSH-responsive MOF for the encapsulation of the immunosuppressive enzyme indoleamine 2,3-dioxygenase (IDO) inhibitor BMS-986205, along with nitric oxide (NO) donor moieties in the form of s-nitrosothiol groups (Fig. 4A).<sup>62</sup> This nanodrug exhibited high T<sub>1</sub> relaxivity, enabling its visualization through magnetic resonance imaging for *in vivo* distribution monitoring. Following accumulation in the tumor tissue *via* the enhanced permeability and retention effect and subsequent internalization into tumor cells, the elevated GSH levels therein initiate sequential reactions with the MOF, leading to nanodrug disassembly and rapid release of the IDO-inhibitory BMS-986205, accompanied by substantial NO production. Consequently, the synergistic action of the IDO inhibitor and NO effectively modulated the immunosuppressive tumor microenvironment, resulting in an increased

number of CD8<sup>+</sup> T cells and a decrease in regulatory T cells, thus promoting highly efficacious immunotherapy.

Hao *et al.* employed click chemistry to incorporate a TME-responsive PD-1 inhibitory polypeptide, AUNP12, featuring a disulfide bond, onto the surface of the MOF.<sup>63</sup> Simultaneously, the photothermal agent indocyanine green (ICG) was encapsulated within the AUNP12-modified nanodrug (ICG-MOF-SSAUNP12) to treat melanoma, as illustrated in Fig. 4B. The utilization of the MOF nanocarrier not only enhanced the stability of ICG but also facilitated effective photothermal therapy for eradicating melanoma cells. Furthermore, high GSH levels in tumor tissues responsively cleave the disulfide bond, resulting in the localized release of AUNP12 at tumor sites. This orchestrated a synergistic approach combining photothermal and immunotherapeutic effects in melanoma (Fig. 4B). Thus, this study highlights the promising prospects of MOF nanocarriers for tumor therapy.

In addition to serving as a stimulus for the TME, hypoxia and a dense ECM pose challenges to several established treatments. Studies have been conducted to overcome these obstacles. Zhang *et al.* presented a versatile nanoplatform for enhanced PDT in cancer treatment by incorporating platinum (Pt) nanozymes into photosensitizer-integrated MOFs.<sup>64</sup> Pt undergoes *in situ* growth on the MOF surface, resulting in the formation of a MOF decorated with Pt nanoparticles (Fig. 5A). The Pt component served as a catalase mimic, engaging in the decomposition of hydrogen peroxide (H<sub>2</sub>O<sub>2</sub>) within the biological milieu to generate oxygen (O<sub>2</sub>). The resulting PCN-224-Pt nanocomposite demonstrated significant PDT efficacy through



Fig. 4 (A) Schematic of GSH responsive metal-organic framework (BMS-SNAP-MOF). Reproduced with permission.<sup>62</sup> Copyright (2022): John Wiley and Sons. (B) Schematic of construction and anti-tumor activity of ICG-MOF-SS-AUNP12 nanoparticles for synergistic photothermal and immunotherapy. Reproduced with permission.<sup>63</sup> Copyright (2023): Frontiers Media SA.





**Fig. 5** Schematic of (A) PCN-224-Pt preparation and (B) PCN-224-Pt use for Enhanced PDT. Photodynamic therapy of PCN-224-Pt by intravenous injection in a subcutaneous tumor model. Reproduced with permission.<sup>64</sup> Copyright (2018): American Chemical Society. (C) Schematic of MOF-supported catalase delivery system for hypoxia mitigation and enhancing PDT. Reproduced with permission.<sup>66</sup> Copyright (2023): American Chemical Society.

the activation of  $O_2$  evolution and light-induced production of cytotoxic singlet oxygen ( $^1O_2$ ). This study explored the intratumoral and intravenous administration of PCN-224-Pt in mouse models and demonstrated its ability to alleviate tumor hypoxia, induce cancer cell damage, and effectively inhibit tumor growth (Fig. 5B). The combination of Pt nanozymes and MOFs is a promising strategy for enhancing the efficiency of PDT with potential applications in modern oncology.

Cheng *et al.* proposed a non-pharmacological platform for cancer treatment that integrates chemodynamic therapy (CDT), PDT, and photothermal therapy (PTT). This strategy aimed to achieve an efficacious and low-toxicity strategy<sup>65</sup> and focused on mitigating tumor hypoxia, a challenge associated with treatment resistance and metastasis. MOFs, specifically Cu/Zn-MOFs, serve as the foundation for constructing a theranostic platform. This platform demonstrated the ability to catalyze  $H_2O_2$  to  $O_2$  and consume GSH, thereby enhancing treatment efficacy. The integration of  $Cu^{2+}$  ions and  $MnO_2$  further augments therapeutic effects. The proposed mixed-metal MOF strategy is emphasized for its simplicity and effectiveness in creating a hollow structure with integrated multifunctionality, ultimately enhancing theranostic performance. The capability of this platform to convert intracellular  $H_2O_2$  into  $O_2$  has been highlighted as an effective approach for alleviating hypoxia and enhancing PDT. This approach circumvents chemotherapy-related toxicity and drug resistance and offers a promising avenue for cancer treatment.

Sim *et al.* explored an innovative strategy to address tumor hypoxia in PDT for cancer treatment by employing MOF nanoparticles for the targeted delivery of the enzyme catalase (CAT) (Fig. 5C).<sup>66</sup> In this study, Zr-based MOF (MOF-808) nanoparticles were employed utilizing supramolecular techniques to facilitate the direct binding of CAT to the MOF surface. This binding occurred through supramolecular chemical interactions, specifically through the coordination bonds formed

between the unsaturated sites of Zr and the carboxylic acid groups of the protein. Notably, this was achieved without additional chemical intervention. Consequently, MOF nanoparticles loaded with CAT demonstrated exceptional oxygen production capabilities under hypoxic conditions, particularly in scenarios where  $H_2O_2$  was decomposed by CAT in the presence of  $H_2O_2$ . The introduction of a photosensitizer (IR780) augments ROS production during PDT. Cellular uptake investigations substantiated the efficient delivery of MOF-CAT to cancer cells, effectively mitigating hypoxia and amplifying ROS production. *In vitro* cytotoxicity assays underscored the therapeutic efficacy of MOF-based delivery systems, particularly in hypoxic environments, indicating that they are a promising avenue for enhancing PDT effectiveness and refining outcomes in cancer therapeutics.

In addition, Liu *et al.* proposed a collagenase scaffold named PMOCOL by combining metal-organic ligands with proteins, utilizing host-guest interactions (Fig. 6A).<sup>67</sup> The complex structure was designed to specifically regulate the ECM in deep tumor regions aiming to enhance immunotherapeutic approaches. To validate its effectiveness, a pancreatic adenocarcinoma model was utilized to take advantage of the abundant ECM and cold immune microenvironments of such tumors. Proteins played a key role in constructing the PMOCOL scaffold, achieving an impressive collagenase encapsulation rate of 80.3% (w/w), surpassing that of previous protein-carrying MOFs. PMOCOL exhibited heightened sensitivity to the acidic conditions of the tumor microenvironment, leading to the release of active collagenase. This facilitates the decomposition of collagen, promotes the penetration of therapeutic agents into the avascular regions, and induces deep-tissue Immunogenic Cell Death (ICD), thereby enhancing immunogenic exposure (Fig. 6B).

Qiao *et al.* introduced a biomimetic nanoplatform aimed at regulating transforming growth factor-beta to normalize the



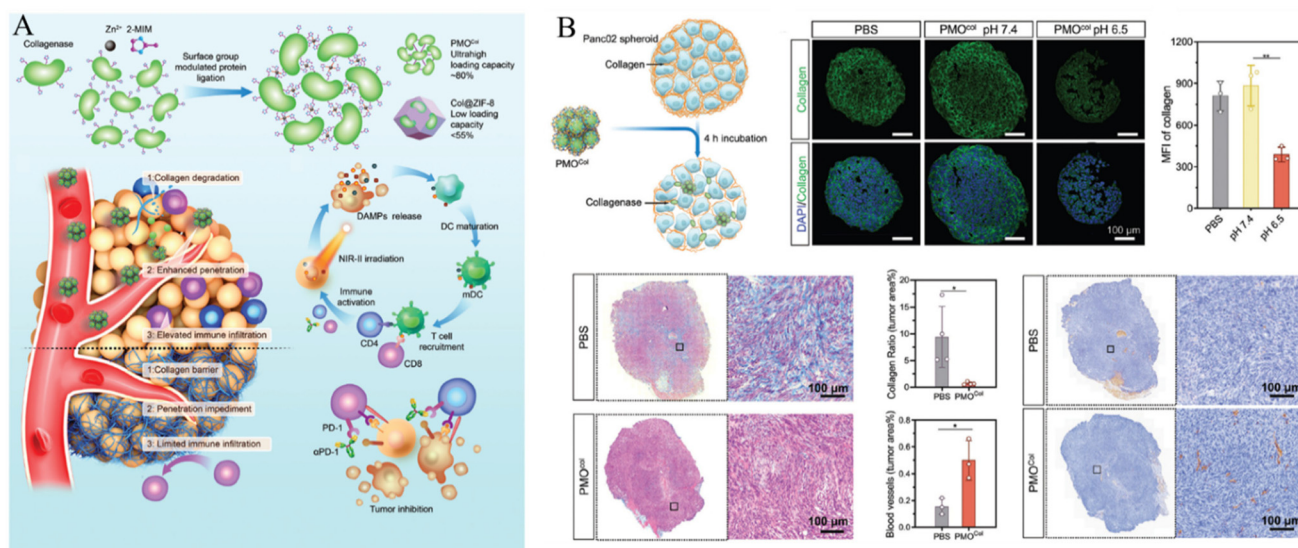


**Fig. 6** (A) Schematic of enzyme-loaded metal–organic framework for deep tissue penetration and (B) enhanced penetration of enzyme-loaded metal–organic framework. Reproduced with permission.<sup>67</sup> Copyright (2023): John Wiley and Sons.

ECM.<sup>68</sup> The nanoplatform utilizes ZIF-8 as a nanocarrier for efficient loading of the chemotherapeutic agent doxorubicin (DOX) and TGFBR1 inhibitor LY364947 (LY). The resulting ZIF-8-DOX-LY nanoparticles were coated with a red blood cell membrane (RM) to form ZIF-8-DOX-LY-RM nanoparticles. These biomimetic nanoparticles demonstrated effective accumulation in tumor tissues, immune escape, and prolonged circulation. In the TME, LY induces structural modifications in the ECM, enhancing nanodrug penetration, and alleviating hypoxia-induced chemoresistance. *In vivo* studies on 4T1 tumor models have highlighted the outstanding performance of the ZIF-8-DOX-LY-RM nanoparticles.



**Fig. 7** Schematic of MOF NPs overcoming cellular internalization.

## Cellular internalization

The cell membrane, which consists of a lipid bilayer, separates and protects the interior of a cell from the outside environment.<sup>34</sup> Nanoparticles struggle to penetrate this barrier through simple diffusion. Therefore, nanoparticles are inserted into cells depending on cell endocytosis.<sup>35–37</sup> Modification of the nanoparticle surface leads to specific interactions with the cell membrane, which can not only induce cellular endocytosis but also inhibit nonspecific cellular internalization of drugs and facilitate selective targeting of cancer.<sup>69</sup> Even if the drug is inserted through the membrane, the drug is expelled out of the cell by the efflux pump in the membrane, which may reduce its efficacy. This phenomenon has led to the development of multidrug resistance (MDR) in cancer cells.<sup>70,71</sup> This chapter describes functionalized materials on the MOF surface and a modification method to overcome cellular internalization, which is a biological barrier (Fig. 7).

The functional groups present in the MOF organic linkers were used for modification. Wang *et al.* developed a system that effectively penetrates the cancer cell membrane using iron (iii)-based MOF MIL-101-N<sub>3</sub> and a polymer functionalized with RGDS and adamantane.<sup>72</sup> MIL-101 (Fe) is widely used as a versatile platform in biomedical applications because it is water-soluble, biocompatible, and degradable. MIL-101-N<sub>3</sub> (Fe) was synthesized from MIL-101-NH<sub>2</sub> (Fe), which contained 2-amino-benzene-1,4-dicarboxylic acid as the organic linker. The amine group of MIL-101-NH<sub>2</sub> (Fe) was converted to an azide by reaction with *tert*-butyl nitrite (*t*BuONO) and trimethylsilane azide (TMSN<sub>3</sub>). The MIL-101-N<sub>3</sub> (Fe) was further modified through strain-promoted azide–alkyne cycloaddition (SPAAC) reaction of bicyclononyne functionalized  $\beta$ -cyclodextrin ( $\beta$ -CD) with the azide group of MIL-101-N<sub>3</sub> (Fe). Polymers consisting of RGDS and adamantane can be easily modified to  $\omega$ - $\beta$ -CD functiona-



lized MOF by the host-guest interaction between  $\beta$ -CD and adamantane. RGDS interacts with  $\alpha\beta$ 3 integrin, which overexpresses cancer cells, allowing MOF to effectively penetrate the cancer cell membrane. To confirm the cancer cell internalization effect, DOX was loaded onto the functionalized MOF and then incubated with  $\alpha\beta$ 3 integrin expression HeLa (human adenocarcinoma) cells<sup>34</sup> and  $\alpha\beta$ 3 integrin negative non-cancerous COS7 (African green monkey kidney) cells, respectively. After incubation, HeLa cells exhibited a 2.5-fold higher fluorescence intensity than COS7 cells, as confirmed by CLSM and flow cytometry.

Gao *et al.* developed a system using MIL-53-NH<sub>2</sub> (Fe) and folic acid.<sup>73</sup> MIL-53-NH<sub>2</sub> (Fe) has intense magnetic properties, which make it an effective magnetic resonance imaging contrast agent. Furthermore, the amino groups on the surface of MIL-53-NH<sub>2</sub> (Fe) formed an amide bond with folic acid, which has a carboxylic acid functional group, facilitating MOF functionalization. The modified folic acid interacts with the folate receptor overexpressed on the cancer cell membrane and induces MOF to penetrate the cancer cell membrane. The functionalized MOFs were incubated with folate receptor-positive MGC-803 cells and folate receptor-negative human aortic smooth muscle cells (HASMC) to confirm cancer cell internalization. After incubation, MGC-803 cells showed higher fluorescence intensity than HASMC.

In addition, Abazari *et al.* developed a folic acid-functionalized MOF system through an amide bond on an amine-functionalized MOF (NH<sub>2</sub>-Eu:TMU-62), (TMU standing for Tarbiat Modares University).<sup>74</sup> Folic acid modified NH<sub>2</sub>-Eu:TMU-62 was incubated with MCF-7 breast cancer cells and MCF-10A normal breast cells after loading with 5-fluorouracil as an anti-cancer drug. Folic acid-modified NH<sub>2</sub>-Eu:TMU-62 showed higher cytotoxicity toward MCF-7 cells than MCF-10A cells. These cytotoxicity data suggest that the interaction between the folate receptor and folic acid increases the cancer cell internalization of drug-loaded MOF.

The coordination bond between the metal active site and the lone pair of electrons was used to modify folic acid on the MOF surface. Zeng *et al.* proposed a facile strategy for the fabrication of a hollow and monodisperse MOF (hMIL-88B(Fe)@ZIF-8).<sup>75</sup> Hollow MIL-88B (hMIL-88B) is created by partial etching of MIL-88B MOF by 2-methylimidazole and Zn<sup>2+</sup> ions adsorbed on the surface of MIL-88B(Fe) coordinate with the 2-MeIm ligand to synthesize another MOF (ZIF-8). ZIF-8 is present on the surface, protects the nanoparticles, and maintains their morphology. hMIL-88B endows its cavity with various materials. Folic acid, which has a carboxylic acid functional group, is modified on hMIL-88B(Fe)@ZIF-8 through coordination bonding. To confirm the effect of folic acid on cancer cell internalization, folic acid-functionalized hMIL-88B (Fe)@ZIF-8 (hMIL-88B (Fe)@ZIF-8@FA), and hMIL-88B (Fe)@ZIF-8 cells were incubated with MCF-7 cells. MCF-7 cells incubated with hMIL-88B (Fe)@ZIF-8@FA showed a stronger intensity than those incubated with hMIL-88B (Fe)@ZIF-8.

Other materials with lone-pair electrons can be modified on the MOF surface *via* coordination bonds. For example, Wang *et al.* developed a system that targets cancer cells and effectively penetrates the cell membrane using ZIF-8 and apoferritin (Aft) (Fig. 8A).<sup>76</sup> ZIF-8 was degraded under acidic conditions. Thus, this property facilitates controlled drug release from the tumor tissue. Aft, which is modified on the surface of the MOF, can selectively react with transferrin receptor 1 (Tfr1) overexpressed in MDA-MB-231 triple-negative breast cancer (TNBC) cells and has its own cage inside the protein, which can serve as another nanocarrier for loading cancer drugs. In addition, it promoted coordination bonding between the N-terminus of the protein and the Zn active site, thereby facilitating protein modification of the MOF surface. The fluorophores were loaded into the synthesized system and incubated with Tfr1-positive MDA-MB-231 cells, Tfr1-negative Mx-1 cancer cells, and normal cells. Their cancer cell internalization effects were confirmed using CLSM imaging and flow



**Fig. 8** (A) Schematic of design and assembly process of the proposed corona-BioMOF nanovehicle and its programmed therapy against breast cancer. Reproduced with permission.<sup>76</sup> Copyright (2023): Elsevier. (B) Schematic of Ce6/Cyt c@ZIF-8/HA synthesis and their applications in cancer cells targeted therapy. Reproduced with permission.<sup>77</sup> Copyright (2020): American Chemical Society.



cytometry. After incubation with the AFT-modified MOF, MDA-MB-231 cells presented an 8-fold higher fluorescence intensity than MX-1 and MCF-10A cells.

Hyaluronic acid (HA), a well-known cancer-targeting material, can be modified into MOF to increase the cancer cell membrane penetration of the MOF. Kim *et al.* developed a cancer membrane-penetrating system using PCN-224 and hyaluronic acid (HA).<sup>18</sup> The Zr-based porphyrinic MOF PCN-224 is robust, biodegradable, has a large surface area, is stable over a wide pH range, and can generate  $^1\text{O}_2$ , an essential feature for PDT. HA a natural biocompatible polysaccharide, interacts with CD44, which is overexpressed in numerous cancer cells. Furthermore, the carboxylic acid group in HA forms multiple coordination bonds with the MOF and facilitates the penetration of the MOF into the cancer membrane. To confirm the cancer cell internalization, DOX-loaded HA-modified PCN-224 (HA-DOX-PCN) was incubated with CD44 negative normal cell (HEK 293T) and CD44 overexpressed carcinoma cell (MDA-MB-231 and SCC-7). After incubation, the cellular uptake ability of HA-DOX-PCNs was observed by confocal microscopy and flow cytometry. The MDAMB231 and SCC-7 cell lines showed a higher intensity of DOX compared to that of the HEK 293T cell line.

Ding *et al.* developed an HA-modified ZIF-8 system.<sup>77</sup> Chlorin e6 (Ce6, a potent PS) and cytochrome c (Cyt c, an apoptosis inducer) were co-encapsulated in ZIF-8 for cancer therapy. HA was functionalized on the ZIF-8 surface by a coordination bond and electrostatic interactions to induce the cancer cell internalization effect of the MOF (Fig. 8B). HA-func-

tionized MOF loaded with a fluorophore were incubated with CD44 negative L929 cells and CD44 positive HeLa cell to confirm cancer cell internalization. After incubation, HeLa cells exhibited higher fluorescence intensity than L929 cells. To further demonstrate the targeting ability of HA, HeLa cells were incubated with free HA to block CD44 receptors. After blocking, fluorescence intensity decreased. This result suggests that the interaction between HA and CD44 receptors increases the cellular internalization of the nanoparticles.

P-glycoprotein (P-gp) plays an important role in MDR by actively transporting structurally diverse compounds out of the cells. Their main function is to excrete cytotoxic drugs, thereby reducing their intracellular concentration and efficacy. Through this mechanism, cancer cells become resistant to chemotherapy.<sup>78</sup> Huang *et al.* developed a P-gp inhibition system to treat MDR cells using a MOF composed of iron ions and 4,4'-azobisbenzoic acid (AMOF) (Fig. 9A).<sup>79</sup> Azobenzenes within the AMOF framework can be reduced to amines by highly expressed azoreductases under oxygen-deficient environments, leading to the release of the encapsulated drug under hypoxic conditions. Additionally, a cancer drug (Dox) is internalized during the MOF synthesis stage, and a double-stranded DNA/RNA hybridization complex (DRHC) composed of HIF-1 $\alpha$  against small interfering RNA (siRNA, RX-0047) is loaded into the AMOF through electrostatic interaction and coordination bonds. HIF-1 $\alpha$  enhances the expression of P-glycoprotein (P-gp), a membrane efflux pump that can transport cancer drugs out of cells, thereby contributing to chemotherapy resistance and reducing the efficacy of the drugs.

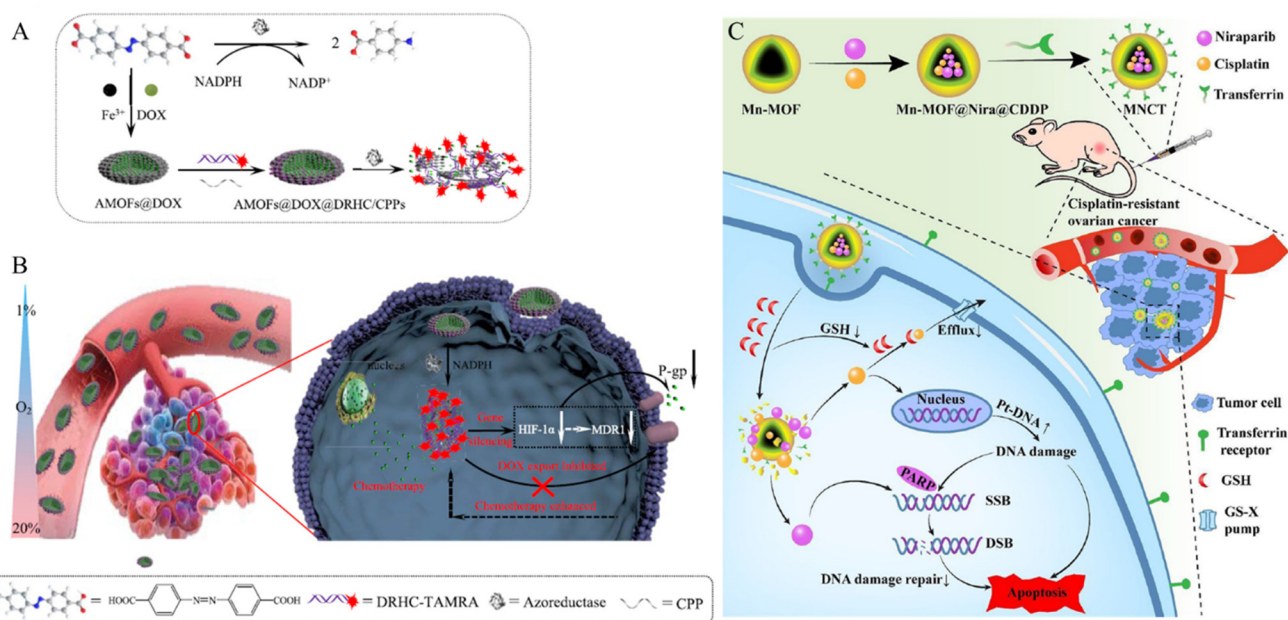


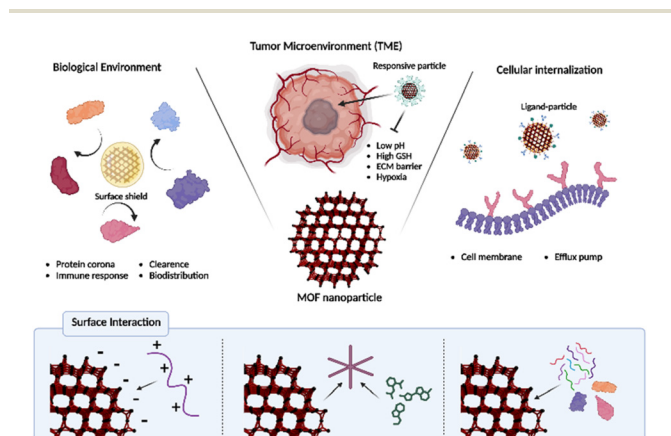
**Fig. 9** (A) Synthesis process and response mechanism for functional metal-organic framework-based nanodrug (DOX@AMOFs@DRHC/CPPs). (B) Cellular functions of DOX@AMOFs@DRHC/CPPs, including azoreductase-responsive DOX and DRHC releasing, downregulation of predictive markers (HIF-1 $\alpha$ , MDR1, and P-gp), inhibited DOX export, and then enhanced chemoresistance for hypoxic tumor. Reproduced with permission.<sup>79</sup> Copyright (2019): American Chemical Society. (C) Schematic of multitargeted nanodrug delivery system Tf-Mn-MOF@Nira@CDDP (MNCT) to co-deliver cisplatin and niraparib on cisplatin-resistant ovarian cancer. Reproduced with permission.<sup>81</sup> Copyright (2023): American Chemical Society.



Thus, HIF-1 $\alpha$  against RX-0047 suppresses this process, overcoming drug resistance and facilitating the MDR cell treatment. The AMOF had a rod-like morphology and was approximately 150 nm in size. By modification with cell-penetrating peptides (CPPs) through electrostatic interactions, a system (DOX@AMOFs@DRHC/CPP) that releases the drug in response to azoreductases and treats MDR cells was synthesized by encapsulating Dox and DRHC in AMOF (Fig. 9B). DOX@AMOFs@DRHC/CPP effectively inhibited the expression

of HIF- $\alpha$  and P-gp. To confirm the therapeutic effects, PBS, DOX@AMOFs@random DNA/CPP, AMOFs@DRHC/CPP, and DOX@AMOFs@DRHC/CPP were injected into tumor-bearing mice. The group treated with DOX@AMOF @DRHC/CPP exhibited the most effective inhibition of cancer cell growth.

Drug efflux pumps export substrates in the form of GSH conjugates or co-transport reduced GSH. Therefore, high levels of GSH in the body reduce the effectiveness of cancer therapy.<sup>80</sup> Liu *et al.* developed a system that decreased GSH levels in the cell to treat drug-resistant cells using a Mn-MOF composed of 1*H*-1,2,4-triazole-3-thiol and manganese (Mn) (Fig. 9C).<sup>81</sup> Mn-MOF reacts with GSH present in cancer cells, leading to its degradation. This reaction reduces the intracellular GSH levels, inhibiting detoxification and efflux pump-mediated drug outflow. The Mn-MOF was loaded with the cancer drug cisplatin (CDDP) and the poly ADP-ribose polymerase (PARPD) inhibitor niraparib (Nira). CDDP creates lesions in DNA, ultimately leading to apoptosis. Nira inhibits the DNA repair enzyme, PARPD, thereby preventing DNA recovery and enhancing the therapeutic effects of CDDP. The stability and biocompatibility of Mn-MOF were enhanced by coating it with bovine serum albumin (BSA). Finally, transferrin (Tf) was modified onto the surface *via* an amide bond with BSA to create a cancer-targeting system (MNCT). To confirm therapeutic effectiveness, saline, CDDP, Nira, Nira-loaded Mn-MOF, CDDP-loaded Mn-MOF, and CMNCT were injected into tumor-bearing mice. The group injected with CMNCT exhibited the most effective suppression of cancer growth.



**Scheme 2** Overcoming biological barriers of functionalized MOFs and surface interactions for MOF functionalization.

**Table 1** Summary of the utilized MOF type, modified material to overcome the biological barrier, and molecular interaction between MOF and modified material

| No. | Biological barrier | MOF type          | Modified material  | Molecular interaction                        | Ref. |
|-----|--------------------|-------------------|--|--|------|
| 1   | Immune system      | ZIF-8             | Extracellular vesicle membrane (EVM)                                   | Coordination interaction                     | 44   |
| 2   | Immune system      | ZIF-8             | Erythrocyte membrane (eM)  | Electrostatic/hydrophilic interaction        | 46   |
| 3   | Clearance          | UiO-66            | 1,2-Dioleoyl- <i>sn</i> -glycero-3-phosphate (DOPA) lipid bilayer (LB) | Coordination interaction                     | 50   |
| 4   | Clearance          | Zr-fum            | Polymer (BPEI, PAMAM, PGlu, PAA, PEG, Tween, PGlu-PSar)                | Coordination interaction                     | 29   |
| 5   | Clearance          | ZIF-8             | 8-arm-PEG-TNB, HA-SH   | Disulfide bond                               | 51   |
| 6   | Protein corona     | PCN-224           | Glutathione S-transferase fused targetable affibody (GST-Afb)          | Coordination interaction                     | 52   |
| 7   | pH-responsive      | ZIF-14            | Responsive polymer   | Coordination bond, electrostatic interaction | 59   |
| 8   | pH-responsive      | MIL-101           | siRNA, HA  | Coordination bond, electrostatic interaction | 61   |
| 9   | GSH-responsive     | PCN/ZIF-67        | siRNA  | Coordination bond, electrostatic interaction | 56   |
| 10  | GSH-responsive     | Cu-BTC MOF        | Drug, polymer  | Covalent bond, electrostatic interaction     | 61   |
| 11  | GSH-responsive     | Zr-TPDC           | Drug, agonist (AUNP12)   | Bioorthogonal chemistry                      | 64   |
| 12  | Hypoxia            | PCN-224           | Pt nanoparticle  | <i>in situ</i> reduction                     | 64   |
| 13  | Hypoxia            | ZIF-90            | Cu <sup>2+</sup> , MnO <sub>2</sub>                                    | Dissolution-regrowth process                 | 65   |
| 14  | Hypoxia            | MOF-808           | Catalase   | Coordination interaction                     | 66   |
| 15  | ECM                | PMO (Protein-MOF) | Collagenase  | Coordination bond                            | 67   |
| 16  | ECM                | ZIF-8             | Red blood cell membrane  | Self-assembly                                | 68   |
| 17  | Cell membrane      | MIL-101-N3(Fe)    | RGDS   | SPAAC, host-guest interaction                | 71   |
| 18  | Cell membrane      | MIL-53-N3(Fe)     | Folic acid   | Amide bond                                   | 73   |
| 19  | Cell membrane      | NH2-Eu:TMU-62     | Folic acid   | Amide bond                                   | 74   |
| 20  | Cell membrane      | MIL-88B, ZIF-8    | Folic acid   | Coordination bond                            | 75   |
| 21  | Cell membrane      | ZIF-8             | Aft  | Coordination bond                            | 76   |
| 22  | Cell membrane      | PCN-224           | Hyaluronic acid  | Coordination bond                            | 18   |
| 23  | Cell membrane      | ZIF-8             | Hyaluronic acid  | Coordination bond, electrostatic interaction | 77   |
| 24  | Efflux pump        | AMOF              | siRNA, CPPs  | Coordination bond, electrostatic interaction | 79   |
| 25  | Efflux pump        | Mn-MOF            | Nira, Tf   | Physical adsorption, amide bond              | 81   |



## Multifunctionality of MOF based system

In the preceding discourse, we introduced many models delineating strategies to surmount biological barriers *via* diverse modifications. In this section, we aim to delve deeper into investigations employing multiple functionalities concurrently. Given our ultimate objective of overcoming biological barriers and eradicating target disease cells, we posit that a more comprehensive discussion encompassing both barrier overcoming and therapeutic interventions could yield additional insights compared to addressing singular functions.<sup>40</sup> For example, in the study by Oh *et al.*, a specifically structured recombinant protein (GST-Afb) was employed to establish a protective shield inducing a stealth effect on the surface while ensuring target functionality. This circumvented the protein corona phenomenon, facilitating targeting, while the pore structure of MOFs and porphyrin linker were utilized for complex therapeutic interventions.<sup>52</sup> In addition, Sim *et al.* successfully navigated hypoxic environments by surface-modifying enzymes (catalase) on MOF nanoparticles to optimize the efficacy of photosensitizers present within the particles' pores.<sup>66</sup> Subsequently, in Kim *et al.*'s investigation, they harnessed a material enabling concurrent gatekeeping and targeting through the utilization of defect sites on particle surfaces, embedding the drug within nanoparticle pore structures to effectuate simultaneous delivery and therapeutic efficacy.<sup>18</sup> This versatility enables the incorporation of multiple functionalities within a single particle through various permutations, thereby significantly contributing to the development of more sophisticated delivery systems.

## Conclusion and outlook

In the preceding discourse, a comprehensive examination was undertaken to elucidate diverse investigations involving MOF nanoparticles and their prospective applications. In summary, the large surface area inherent in MOFs facilitates the adsorption of diverse guest molecules, thereby enhancing drug delivery efficacy. Moreover, the distinctive properties of MOFs facilitate the development of stimuli-responsive systems and integrated cancer therapies. Noteworthy biological barriers, including bio-clearance, TME, and cellular internalization, pose significant challenges not only in traditional cancer treatments utilizing other nanomedicines but also in MOF-based systems, thereby influencing the effectiveness of cancer therapy. The bioclearance system actively eliminates therapeutically injected nanoparticles *via* organs, the immune system, and the protein corona. Addressing this challenge involves leveraging materials evading clearance systems such as cell membrane polymers and proteins. The TME, a complex ecosystem surrounding tumors, presents specific properties, such as pH and GSH, which can serve as triggers in cancer treatment. Overcoming challenges such as hypoxia and dense ECM involves modifications utilizing catalase, nanoparticles, and folic acid. Cell

membranes play a crucial role in protecting the cells from external stimuli and preventing indiscriminate nanoparticle penetration. Successful therapeutic intervention requires the insertion of drugs into the cells for effective cancer therapy. This obstacle to cellular internalization is overcome through ligand modification, which selectively interacts with receptors overexpressed on cancer cells on the MOF surface. Scheme 2 and Table 1 summarizes MOF-based nanomedicines, highlighting their functionalization to overcome biological barriers. Additionally, as indicated in this review, enhancing the therapeutic effects of nanomedicine involves escaping various biological barriers through relatively straightforward surface functionalization. In conclusion, this manuscript provides an insightful exploration into the manifold capabilities of MOF nanoparticle systems. However, the transition of these systems into successful clinical trials hinges upon overcoming several challenges. Foremost among these is ensuring the stability and sustained functionality of MOF-based drug delivery platforms within biological environments, a task fraught with complexity. Ongoing research endeavors are directed towards fortifying MOF stability against degradation, employing strategies encompassing rational linker and node chemistry design, encapsulation within protective matrices, and optimization of synthesis methodologies. Furthermore, achieving precise *in vivo* targeting poses a significant obstacle, necessitating advancements in ligand specificity, optimization of pharmacokinetic profiles, and circumvention of biological barriers impeding tissue penetration. Additionally, the critical evaluation of immunogenicity and biocompatibility underscores the imperative to ensure the safety and seamless integration of MOF-based drug delivery systems with biological matrices. Rigorous preclinical assessments encompassing immune responses, biocompatibility profiles, and long-term biodegradation kinetics are essential to mitigate potential adverse effects and facilitate regulatory approval for clinical translation. Addressing these challenges demands interdisciplinary collaboration among researchers, clinicians, and engineers to harness the full potential of MOF-based drug delivery systems and realize their clinical utility. Despite the hurdles ahead, the future prospects for MOF-based drug delivery systems remain promising, poised to revolutionize drug delivery and enhance patient outcomes across diverse therapeutic domains.

## Author contributions

Jun Yong Oh: Writing – original draft, writing – review & editing; Youjung Sim: writing – original draft, writing – review & editing; Gyeongseok Yang: writing – original draft, writing – review & editing; Myoung-Hwan Park: supervision, writing – review & editing; Kibeom Kim: supervision, writing – original draft, writing – review & editing; Ja-Hyoung Ryu: conceptualization, supervision, writing – review & editing, funding acquisition.



## Conflicts of interest

There are no conflicts to declare.

## Acknowledgements

This work was supported by Basic Science Research Program through the National Research Foundation of Korea (NRF) funded by the Korean Government (MSIT) (RS-2023-00281553, RS-2023-00208386, 2020M3A9D8038192, 2022R1F1A1068232, RS-2023-00255698, and 2022R1A6A3A01085939).

## References

- S. N. Bhatia, X. Chen, M. A. Dobrovolskaia and T. Lammers, Cancer nanomedicine, *Nat. Rev. Cancer*, 2022, **22**, 550–556.
- H. D. Lawson, S. P. Walton and C. Chan, Metal-Organic Frameworks for Drug Delivery: A Design Perspective, *ACS Appl. Mater. Interfaces*, 2021, **13**, 7004–7020.
- C. A. Moreno-Camacho, J. R. Montoya-Torres, A. Jaegler and N. Gondran, Sustainability metrics for real case applications of the supply chain network design problem: A systematic literature review, *J. Cleaner Prod.*, 2019, **231**, 600–618.
- Z. Shi, Y. Zhou, T. Fan, Y. Lin, H. Zhang and L. Mei, Inorganic nano-carriers based smart drug delivery systems for tumor therapy, *Smart Mater. Med.*, 2020, **1**, 32–47.
- J. Y. Oh, E.-K. An, B. Jana, H. Kim, S. Jin, G. Yang, J. Kim, E. Choi, J.-O. Jin and J.-H. Ryu, Antibody plug-and-playable nanoparticles as a facile and versatile platform for targeted drug delivery, *Chem. Eng. J.*, 2023, **470**, 144357.
- C. S. L. Koh, H. Y. F. Sim, S. X. Leong, S. K. Boong, C. Chong and X. Y. Ling, Plasmonic Nanoparticle-Metal-Organic Framework (NP-MOF) Nanohybrid Platforms for Emerging Plasmonic Applications, *ACS Mater. Lett.*, 2021, **3**, 557–573.
- S. T. Meek, J. A. Greathouse and M. D. Allendorf, Metal-organic frameworks: a rapidly growing class of versatile nanoporous materials, *Adv. Mater.*, 2011, **23**, 249–267.
- R. Roder, T. Preiss, P. Hirschle, B. Steinborn, A. Zimpel, M. Hohn, J. O. Radler, T. Bein, E. Wagner, S. Wuttke and U. Lachelt, Multifunctional Nanoparticles by Coordinative Self-Assembly of His-Tagged Units with Metal-Organic Frameworks, *J. Am. Chem. Soc.*, 2017, **139**, 2359–2368.
- J. Yu, C. Mu, B. Yan, X. Qin, C. Shen, H. Xue and H. Pang, Nanoparticle/MOF composites: preparations and applications, *Mater. Horiz.*, 2017, **4**, 557–569.
- M. Durymanov, A. Permyakova, S. Sene, A. Guo, C. Kroll, M. Gimenez-Marques, C. Serre and J. Reineke, Cellular Uptake, Intracellular Trafficking, and Stability of Biocompatible Metal-Organic Framework (MOF) Particles in Kupffer Cells, *Mol. Pharm.*, 2019, **16**, 2315–2325.
- Y. Han, S. Zhang, N. Shen, D. Li and X. Li, MOF-derived porous NiO nanoparticle architecture for high performance supercapacitors, *Mater. Lett.*, 2017, **188**, 1–4.
- G. Hu, L. Yang, Y. Li and L. Wang, Continuous and scalable fabrication of stable and biocompatible MOF@SiO<sub>2</sub> nanoparticles for drug loading, *J. Mater. Chem. B*, 2018, **6**, 7936–7942.
- P. Jin, W. Tan, J. Huo, T. Liu, Y. Liang, S. Wang and D. Bradshaw, Hierarchically porous MOF/polymer composites via interfacial nanoassembly and emulsion polymerization, *J. Mater. Chem. A*, 2018, **6**, 20473–20479.
- D. H. Yang, T. T. T. Nguyen, S. T. Navale, L. H. T. Nguyen, Y. T. Dang, N. X. D. Mai, T. B. Phan, J.-Y. Kim, T. L. H. Doan, S. S. Kim and H. W. Kim, Novel amine-functionalized zinc-based metal-organic framework for low-temperature chemiresistive hydrogen sensing, *Sens. Actuators, B*, 2022, **368**, 132120.
- C. Orellana-Tavra, E. F. Baxter, T. Tian, T. D. Bennett, N. K. Slater, A. K. Cheetham and D. Fairen-Jimenez, Amorphous metal-organic frameworks for drug delivery, *Chem. Commun.*, 2015, **51**, 13878–13881.
- J. W. M. Osterrieth and D. Fairen-Jimenez, Metal-Organic Framework Composites for Theragnostics and Drug Delivery Applications, *Biotechnol. J.*, 2021, **16**, e2000005.
- J. Yang and Y. W. Yang, Metal-organic framework-based cancer theranostic nanoplatfoms, *View*, 2020, **1**, 2.
- K. Kim, S. Lee, E. Jin, L. Palanikumar, J. H. Lee, J. C. Kim, J. S. Nam, B. Jana, T. H. Kwon, S. K. Kwak, W. Choe and J. H. Ryu, MOF x Biopolymer: Collaborative Combination of Metal-Organic Framework and Biopolymer for Advanced Anticancer Therapy, *ACS Appl. Mater. Interfaces*, 2019, **11**, 27512–27520.
- J. Park, Q. Jiang, D. Feng, L. Mao and H. C. Zhou, Size-Controlled Synthesis of Porphyrinic Metal-Organic Framework and Functionalization for Targeted Photodynamic Therapy, *J. Am. Chem. Soc.*, 2016, **138**, 3518–3525.
- I. Abánades Lázaro, S. Haddad, J. M. Rodrigo-Muñoz, R. J. Marshall, B. Sastre, V. del Pozo, D. Fairen-Jimenez and R. S. Forgan, Surface-Functionalization of Zr-Fumarate MOF for Selective Cytotoxicity and Immune System Compatibility in Nanoscale Drug Delivery, *ACS Appl. Mater. Interfaces*, 2018, **10**, 31146–31157.
- S. Wang, W. Morris, Y. Liu, C. M. McGuirk, Y. Zhou, J. T. Hupp, O. K. Farha and C. A. Mirkin, Surface-Specific Functionalization of Nanoscale Metal-Organic Frameworks, *Angew. Chem., Int. Ed.*, 2015, **54**, 14738–14742.
- W. Morris, W. E. Briley, E. Auyeung, M. D. Cabezas and C. A. Mirkin, Nucleic acid-metal organic framework (MOF) nanoparticle conjugates, *J. Am. Chem. Soc.*, 2014, **136**, 7261–7264.
- W. Cai, H. Gao, C. Chu, X. Wang, J. Wang, P. Zhang, G. Lin, W. Li, G. Liu and X. Chen, Engineering Phototheranostic Nanoscale Metal-Organic Frameworks for Multimodal Imaging-Guided Cancer Therapy, *ACS Appl. Mater. Interfaces*, 2017, **9**, 2040–2051.



- 24 V. R. Cherkasov, E. N. Mochalova, A. V. Babenyshev, J. M. Rozenberg, I. L. Sokolov and M. P. Nikitin, Antibody-directed metal-organic framework nanoparticles for targeted drug delivery, *Acta Biomater.*, 2020, **103**, 223–236.
- 25 C. He, K. Lu, D. Liu and W. Lin, Nanoscale metal-organic frameworks for the co-delivery of cisplatin and pooled siRNAs to enhance therapeutic efficacy in drug-resistant ovarian cancer cells, *J. Am. Chem. Soc.*, 2014, **136**, 5181–5184.
- 26 Y. Liu, W. Hou, L. Xia, C. Cui, S. Wan, Y. Jiang, Y. Yang, Q. Wu, L. Qiu and W. Tan, ZrMOF nanoparticles as quenchers to conjugate DNA aptamers for target-induced bioimaging and photodynamic therapy, *Chem. Sci.*, 2018, **9**, 7505–7509.
- 27 K. Ni, T. Luo, A. Culbert, M. Kaufmann, X. Jiang and W. Lin, Nanoscale Metal-Organic Framework Co-delivers TLR-7 Agonists and Anti-CD47 Antibodies to Modulate Macrophages and Orchestrate Cancer Immunotherapy, *J. Am. Chem. Soc.*, 2020, **142**, 12579–12584.
- 28 Z. Wang, Y. Fu, Z. Kang, X. Liu, N. Chen, Q. Wang, Y. Tu, L. Wang, S. Song, D. Ling, H. Song, X. Kong and C. Fan, Organelle-Specific Triggered Release of Immunostimulatory Oligonucleotides from Intrinsically Coordinated DNA-Metal-Organic Frameworks with Soluble Exoskeleton, *J. Am. Chem. Soc.*, 2017, **139**, 15784–15791.
- 29 A. Zimpel, N. Al Danaf, B. Steinborn, J. Kuhn, M. Hohn, T. Bauer, P. Hirschle, W. Schrimpf, H. Engelke, E. Wagner, M. Barz, D. C. Lamb, U. Lachelt and S. Wuttke, Coordinative Binding of Polymers to Metal-Organic Framework Nanoparticles for Control of Interactions at the Biointerface, *ACS Nano*, 2019, **13**, 3884–3895.
- 30 A. Wang, M. Walden, R. Ettlinger, F. Kiessling, J. J. Gassensmith, T. Lammers, S. Wuttke and Q. Peña, Biomedical metal-organic framework materials: perspectives and challenges, *Adv. Funct. Mater.*, 2023, 2308589.
- 31 A. E. Nel, L. Madler, D. Velegol, T. Xia, E. M. Hoek, P. Somasundaran, F. Klaessig, V. Castranova and M. Thompson, Understanding biophysicochemical interactions at the nano-bio interface, *Nat. Mater.*, 2009, **8**, 543–557.
- 32 M. V. Zyuzin, Y. Yan, R. Hartmann, K. T. Gause, M. Nazareus, J. Cui, F. Caruso and W. J. Parak, Role of the Protein Corona Derived from Human Plasma in Cellular Interactions between Nanoporous Human Serum Albumin Particles and Endothelial Cells, *Bioconjugate Chem.*, 2017, **28**, 2062–2068.
- 33 M. Jia, D. Zhang, C. Zhang and C. Li, Nanoparticle-based delivery systems modulate the tumor microenvironment in pancreatic cancer for enhanced therapy, *J. Nanobiotechnol.*, 2021, **19**, 384.
- 34 M. Z. Jin and W. L. Jin, The updated landscape of tumor microenvironment and drug repurposing, *Signal Transduction Targeted Ther.*, 2020, **5**, 166.
- 35 A. Tiwari, R. Trivedi and S. Y. Lin, Tumor microenvironment: barrier or opportunity towards effective cancer therapy, *J. Biomed. Sci.*, 2022, **29**, 83.
- 36 W. L. Liu, M. Z. Zou, S. Y. Qin, Y. J. Cheng, Y. H. Ma, Y. X. Sun and X. Z. Zhang, Recent Advances of Cell Membrane-Coated Nanomaterials for Biomedical Applications, *Adv. Funct. Mater.*, 2020, **30**, 2003559.
- 37 A. Akinc and G. Battaglia, Exploiting endocytosis for nanomedicines, *Cold Spring Harbor Perspect. Biol.*, 2013, **5**, a016980.
- 38 B. Li and L. A. Lane, Probing the biological obstacles of nanomedicine with gold nanoparticles, *Wiley Interdiscip. Rev.: Nanomed. Nanobiotechnol.*, 2019, **11**, e1542.
- 39 E. Ruoslahti, S. N. Bhatia and M. J. Sailor, Targeting of drugs and nanoparticles to tumors, *J. Cell Biol.*, 2010, **188**, 759–768.
- 40 R. Freund, U. Lächelt, T. Gruber, B. Rühle and S. Wuttke, Multifunctional efficiency: extending the concept of atom economy to functional nanomaterials, *ACS Nano*, 2018, **12**, 2094–2105.
- 41 M. J. Mitchell, M. M. Billingsley, R. M. Haley, M. E. Wechsler, N. A. Peppas and R. Langer, Engineering precision nanoparticles for drug delivery, *Nat. Rev. Drug Discovery*, 2021, **20**, 101–124.
- 42 I. de Lazaro and D. J. Mooney, Obstacles and opportunities in a forward vision for cancer nanomedicine, *Nat. Mater.*, 2021, **20**, 1469–1479.
- 43 Z. Zhang, Q. Deng, C. Xiao, Z. Li and X. Yang, Rational Design of Nanotherapeutics Based on the Five Features Principle for Potent Elimination of Cancer Stem Cells, *Acc. Chem. Res.*, 2022, **55**, 526–536.
- 44 G. Cheng, W. Li, L. Ha, X. Han, S. Hao, Y. Wan, Z. Wang, F. Dong, X. Zou, Y. Mao and S. Y. Zheng, Self-Assembly of Extracellular Vesicle-like Metal-Organic Framework Nanoparticles for Protection and Intracellular Delivery of Biofunctional Proteins, *J. Am. Chem. Soc.*, 2018, **140**, 7282–7291.
- 45 S. Kamerkar, V. S. LeBleu, H. Sugimoto, S. Yang, C. F. Ruivo, S. A. Melo, J. J. Lee and R. Kalluri, Exosomes facilitate therapeutic targeting of oncogenic KRAS in pancreatic cancer, *Nature*, 2017, **546**, 498–503.
- 46 L. Zhang, Z. Wang, Y. Zhang, F. Cao, K. Dong, J. Ren and X. Qu, Erythrocyte Membrane Cloaked Metal-Organic Framework Nanoparticle as Biomimetic Nanoreactor for Starvation-Activated Colon Cancer Therapy, *ACS Nano*, 2018, **12**, 10201–10211.
- 47 R. S. Franco, Measurement of red cell lifespan and aging, *Transfus. Med. Hemother.*, 2012, **39**, 302–307.
- 48 P. C. Ke, S. Lin, W. J. Parak, T. P. Davis and F. Caruso, A Decade of the Protein Corona, *ACS Nano*, 2017, **11**, 11773–11776.
- 49 X. Bai, J. Wang, Q. Mu and G. Su, In vivo Protein Corona Formation: Characterizations, Effects on Engineered Nanoparticles' Biobehaviors, and Applications, *Front. Bioeng. Biotechnol.*, 2021, **9**, 646708.
- 50 R. Zhang, C. Qiao, Q. Jia, Y. Wang, H. Huang, W. Chang, H. Wang, H. Zhang and Z. Wang, Highly Stable and Long-Circulating Metal-Organic Frameworks Nanoprobes for Sensitive Tumor Detection In Vivo, *Adv. Healthc. Mater.*, 2019, **8**, e1900761.



- 51 Y. Tian, Z. Gao, N. Wang, M. Hu, Y. Ju, Q. Li, F. Caruso, J. Hao and J. Cui, Engineering Poly(ethylene glycol) Nanoparticles for Accelerated Blood Clearance Inhibition and Targeted Drug Delivery, *J. Am. Chem. Soc.*, 2022, **144**, 18419–18428.
- 52 J. Y. Oh, E. Choi, B. Jana, E. M. Go, E. Jin, S. Jin, J. Lee, J. H. Bae, G. Yang, S. K. Kwak, W. Choe and J. H. Ryu, Protein-Precoated Surface of Metal-Organic Framework Nanoparticles for Targeted Delivery, *Small*, 2023, **19**, e2300218.
- 53 Y. Yan and H. Ding, pH-Responsive Nanoparticles for Cancer Immunotherapy: A Brief Review, *Nanomaterials*, 2020, **10**, 1613.
- 54 S. Uthaman, K. M. Huh and I. K. Park, Tumor microenvironment-responsive nanoparticles for cancer theragnostic applications, *Biomater. Res.*, 2018, **22**, 22.
- 55 Q. He, J. Chen, J. Yan, S. Cai, H. Xiong, Y. Liu, D. Peng, M. Mo and Z. Liu, Tumor microenvironment responsive drug delivery systems, *Asian J. Pharm. Sci.*, 2020, **15**, 416–448.
- 56 J. Liu, B. J. Córdova Wong, T. Liu, H. Yang, L. Y. Ye and J. Lei, Glutathione-Responsive Heterogeneous Metal-Organic Framework Hybrids for Photodynamic-Gene Synergetic Cell Apoptosis, *Chemistry*, 2022, **28**, e202200305.
- 57 M. Binnewies, E. W. Roberts, K. Kersten, V. Chan, D. F. Fearon, M. Merad, L. M. Coussens, D. I. Gabrilovich, S. Ostrand-Rosenberg, C. C. Hedrick, R. H. Vonderheide, M. J. Pittet, R. K. Jain, W. Zou, T. K. Howcroft, E. C. Woodhouse, R. A. Weinberg and M. F. Krummel, Understanding the tumor immune microenvironment (TIME) for effective therapy, *Nat. Med.*, 2018, **24**, 541–550.
- 58 H. Fan and Z. Guo, Tumor microenvironment-responsive manganese-based nanomaterials for cancer treatment, *Coord. Chem. Rev.*, 2023, **480**, 215027.
- 59 R. Cheng, L. Jiang, H. Gao, Z. Liu, E. Makila, S. Wang, Q. Saïding, L. Xiang, X. Tang, M. Shi, J. Liu, L. Pang, J. Salonen, J. Hirvonen, H. Zhang, W. Cui, B. Shen and H. A. Santos, A pH-Responsive Cluster Metal-Organic Framework Nanoparticle for Enhanced Tumor Accumulation and Antitumor Effect, *Adv. Mater.*, 2022, **34**, e2203915.
- 60 T. Hompland, C. S. Fjeldbo and H. Lyng, Tumor Hypoxia as a Barrier in Cancer Therapy: Why Levels Matter, *Cancers*, 2021, **13**, 499.
- 61 Z. J. Zhang, Y. K. Hou, M. W. Chen, X. Z. Yu, S. Y. Chen, Y. R. Yue, X. T. Guo, J. X. Chen and Q. Zhou, A pH-responsive metal-organic framework for the co-delivery of HIF-2 $\alpha$  siRNA and curcumin for enhanced therapy of osteoarthritis, *J. Nanobiotechnol.*, 2023, **21**, 18.
- 62 L. Du., H. He, Z. Xiao, H. Xiao, Y. An, H. Zhong, M. Lin, X. Meng, S. Han and X. Shuai, GSH-Responsive Metal-Organic Framework for Intratumoral Release of NO and IDO Inhibitor to Enhance Antitumor Immunotherapy, *Small*, 2022, **18**, e2107732.
- 63 Y. Hao, T. Liu, H. Zhou, J. Peng, K. Li and Y. Chen, The GSH responsive indocyanine green loaded PD-1 inhibitory polypeptide AUNP12 modified MOF nanoparticles for photothermal and immunotherapy of melanoma, *Front. Bioeng. Biotechnol.*, 2023, **11**, 1294074.
- 64 Y. Zhang, F. Wang, C. Liu, Z. Wang, L. Kang, Y. Huang, K. Dong, J. Ren and X. Qu, Nanozyme Decorated Metal-Organic Frameworks for Enhanced Photodynamic Therapy, *ACS Nano*, 2018, **12**, 651–661.
- 65 Y. Cheng, C. Wen, Y. Q. Sun, H. Yu and X. B. Yin, Mixed-Metal MOF-Derived Hollow Porous Nanocomposite for Trimodality Imaging Guided Reactive Oxygen Species-Augmented Synergistic Therapy, *Adv. Funct. Mater.*, 2021, **31**, 2104378.
- 66 Y. Sim, J. Seong, S. Lee, D. Kim, E. Choi, M. S. Lah and J. H. Ryu, Metal-Organic Framework-Supported Catalase Delivery for Enhanced Photodynamic Therapy via Hypoxia Mitigation, *ACS Appl. Mater. Interfaces*, 2023, **15**, 50953–50961.
- 67 Q. Liu, L. Wang, Y. Su, W. Dong, H. Wang, Y. Liu, H. Liu, L. Liu and Y. Wang, Ultrahigh Enzyme Loading Metal-Organic Frameworks for Deep Tissue Pancreatic Cancer Photoimmunotherapy, *Small*, 2023, e2305131, DOI: [10.1002/smll.202305131](https://doi.org/10.1002/smll.202305131).
- 68 C. Qiao, X. Wang, G. Liu, Z. Yang, Q. Jia, L. Wang, R. Zhang, Y. Xia, Z. Wang and Y. Yang, Erythrocyte Membrane Camouflaged Metal-Organic Framework Nanodrugs for Remodeled Tumor Microenvironment and Enhanced Tumor Chemotherapy, *Adv. Funct. Mater.*, 2021, **32**, 2107791.
- 69 M. Yu and J. Zheng, Clearance pathways and tumor targeting of imaging nanoparticles, *ACS Nano*, 2015, **9**, 6655–6674.
- 70 K. Moitra, H. Lou and M. Dean, Multidrug efflux pumps and cancer stem cells: insights into multidrug resistance and therapeutic development, *Clin. Pharmacol. Ther.*, 2011, **89**, 491–502.
- 71 G. Zaman, M. Flens, M. Van Leusden, M. De Haas, H. Mülder, J. Lankelma, H. Pinedo, R. Scheper, F. Baas and H. Broxterman, The human multidrug resistance-associated protein MRP is a plasma membrane drug-efflux pump, *Proc. Natl. Acad. Sci. U. S. A.*, 1994, **91**, 8822–8826.
- 72 X. G. Wang, Z. Y. Dong, H. Cheng, S. S. Wan, W. H. Chen, M. Z. Zou, J. W. Huo, H. X. Deng and X. Z. Zhang, A multifunctional metal-organic framework based tumor targeting drug delivery system for cancer therapy, *Nanoscale*, 2015, **7**, 16061–16070.
- 73 X. Gao, M. Zhai, W. Guan, J. Liu, Z. Liu and A. Damirin, Controllable Synthesis of a Smart Multifunctional Nanoscale Metal-Organic Framework for Magnetic Resonance/Optical Imaging and Targeted Drug Delivery, *ACS Appl. Mater. Interfaces*, 2017, **9**, 3455–3462.
- 74 R. Abazari, F. Ataei, A. Morsali, A. M. Z. Slawin and C. L. Carpenter-Warren, A Luminescent Amine-Functionalized Metal-Organic Framework Conjugated with Folic Acid as a Targeted Biocompatible pH-Responsive Nanocarrier for Apoptosis Induction in Breast Cancer Cells, *ACS Appl. Mater. Interfaces*, 2019, **11**, 45442–45454.



- 75 X. Zeng, B. Chen, Y. Song, X. Lin, S. F. Zhou and G. Zhan, Fabrication of Versatile Hollow Metal-Organic Framework Nanoplatfoms for Folate-Targeted and Combined Cancer Imaging and Therapy, *ACS Appl. Bio Mater.*, 2021, **4**, 6417–6429.
- 76 H. Wang, S. Li, L. Wang, Z. Liao, H. Zhang, T. Wei and Z. Dai, Functionalized biological metal-organic framework with nanosized coronal structure and hierarchical wrapping pattern for enhanced targeting therapy, *Chem. Eng. J.*, 2023, **456**, 140963.
- 77 L. Ding, X. Lin, Z. Lin, Y. Wu, X. Liu, J. Liu, M. Wu, X. Zhang and Y. Zeng, Cancer Cell-Targeted Photosensitizer and Therapeutic Protein Co-Delivery Nanoplatfom Based on a Metal-Organic Framework for Enhanced Synergistic Photodynamic and Protein Therapy, *ACS Appl. Mater. Interfaces*, 2020, **12**, 36906–36916.
- 78 S. Modok, H. R. Mellor and R. Callaghan, Modulation of multidrug resistance efflux pump activity to overcome chemoresistance in cancer, *Curr. Opin. Pharmacol.*, 2006, **6**, 350–354.
- 79 C. Huang, W. Tan, J. Zheng, C. Zhu, J. Huo and R. Yang, Azoreductase-Responsive Metal-Organic Framework-Based Nanodrug for Enhanced Cancer Therapy via Breaking Hypoxia-induced Chemoresistance, *ACS Appl. Mater. Interfaces*, 2019, **11**, 25740–25749.
- 80 A. Sau, F. P. Tregno, F. Valentino, G. Federici and A. M. Caccuri, Glutathione transferases and development of new principles to overcome drug resistance, *Arch. Biochem. Biophys.*, 2010, **500**, 116–122.
- 81 Y. Liu, Y. Wang, X. Guan, Q. Wu, M. Zhang, P. Cui, C. Wang, X. Chen, X. Meng and T. Ma, Reversal of Cisplatin Resistance in Ovarian Cancer by the Multitargeted Nanodrug Delivery System Tf-Mn-MOF@Nira@CDDP, *ACS Appl. Mater. Interfaces*, 2023, **15**, 26484–26495.

